Finite-element modelling of fully-coupled active systems involving poroelasticity, piezoelectricity, elasticity, and acoustics

Tomasz G. Zieliński

Department of Intelligent Technologies, Institute of Fundamental Technological Research
ul. Pawińskiego 5B, 02-106 Warsaw, Poland
e-mail: tzielins@ippt.gov.pl

Abstract

The paper discusses some issues concerning fully-coupled finite-element modelling of active-passive systems for vibroacoustic attenuation, involving porous, piezoelectric, and elastic materials, as well as "acoustic" (inviscid) fluids. For porous materials, the advanced, bi-phasic model of poroelasticity is used, which allows to consider elastic vibrations of solid skeleton important at lower frequencies and for porous composites with active inclusions. A discrete finite-element model suitable for analysis of such multiphysics problems is briefly explained. The model is derived (using the Galerkin method) from the variational formulation of coupled problems of poroelasticity, piezoelectricity, elasticity, and acoustics. Finally, some relevant results obtained from a numerical analysis of a disk of active sandwich panel with poroelastic core, fitted into an acoustic waveguide, are presented.

Keywords: acoustics, porous media, smart materials, vibrations, coupled fields, finite element methods, numerical analysis, elasticity
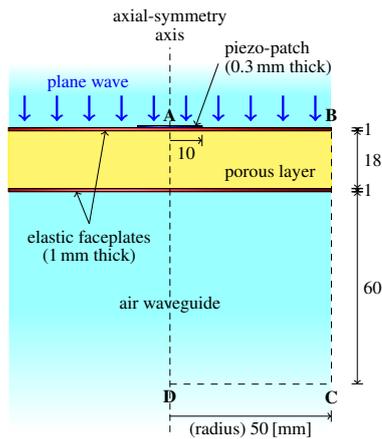
Figure 1: An axially-symmetric disk of active sandwich panel

Figure 2: Discrete model for coupled problems involving poroealsticity, piezoelectricity, elasticity, and acoustics

1. Introduction

An advanced modelling to study hybrid, active/passive vibroacoustic attenuators have been recently proposed [5, 14, 19]. Such attenuators are smart acoustic panels (see Fig. 1), liners and composites which utilize an active approach as a remedy for lack of performance at low frequency, and provide excellent passive absorption at medium and high frequencies, possibly exploiting also the effect based on the combination of both approaches. This paper discusses some issues concerning a fully-coupled finite-element modelling of such active-passive systems for vibroacoustic attenuation, involving poroelastic, piezoelectric, and elastic materials, as well as "acoustic" (inviscid) fluids. The corresponding fully-coupled multiphysics system which will be briefly recalled here, has been recently proposed in [19]. Finally, some relevant results obtained from a numerical analysis of a disk of active sandwich panel with poroelastic core, fitted into an acoustic waveguide, will be presented. The complete results and discussion are going to be published in [20].

2. Fully-coupled finite-element model for active/passive vibroacoustic attenuation

Figure 2 shows a diagram of the discrete system of equations (derived using the Galerkin method) [19] suitable for problems of active/passive vibroacoustics. It combines the following relevant theoretical models: (a) the Biot's theory of poroelasticity [2] – to model the vibroacoustic transmission and passive dissipation of acoustic waves in porous layers, (b) the linear acoustics – to model the propagation of acoustic waves in the surrounding air, air-gaps and waveguides, (c) the linear elasticity – to model the vibrations of elastic faceplates and inclusions, (d) the theory of piezoelectricity [6] – to model the piezoelectric actuators and active control of low-frequency vibrations. For porous materials, the advanced, bi-phasic model of poroelasticity [2] is used, which allows to consider elastic vibrations of solid skeleton important at lower frequencies and for porous composites with active inclusions. The mixed *displacement-pressure* time-harmonic formulation [3] of poroelasticity is used – which requires only 4 DOFs per
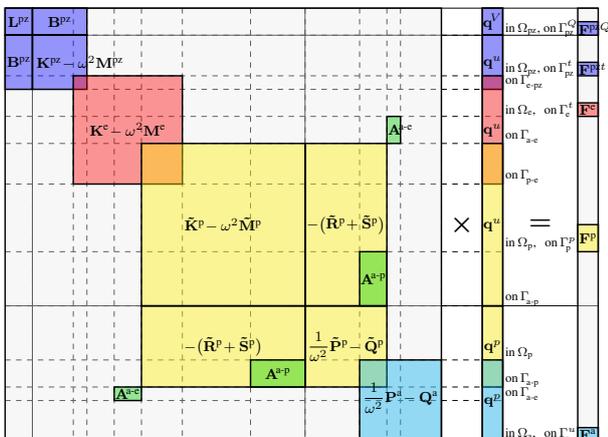
node (instead of 6 required by the original formulation) – in an enhanced version of its weak integral form, which allows to handle easily some boundary and interface-coupling conditions [3]. Some fundamentals of the Biot's theory of poroelasticity will be explained in Sec. 3. The summation convention will be used for (dummy) indices $i, j, k, l = 1, 2, 3$, and the (invariant) differentiation symbol which, in the Cartesian coordinate system, simply reads: $(.)_{|i} = \frac{\partial(.)}{\partial x_i}$.

The discrete multiphysics system was constructed using the following weak integral [19]:

$$\mathcal{WF} = \mathcal{WF}_{\mathrm{p}} + \mathcal{WF}_{\mathrm{e}} + \mathcal{WF}_{\mathrm{pz}} + \mathcal{WF}_{\mathrm{a}} + \mathcal{CI} \,, \tag{1}$$

where $\mathcal{WF}_{\mathrm{p}}$, $\mathcal{WF}_{\mathrm{e}}$, $\mathcal{WF}_{\mathrm{pz}}$, $\mathcal{WF}_{\mathrm{a}}$ are the weak forms of poroelasticity, elasticity, piezoelectricity, and acoustics, respectively, whereas $\mathcal{CI}$ is the coupling integral on the interfaces between various media; all the weak forms are presented below in Sec. 4, and in [19], where the coupling integral is also discussed.

Different materials and media are supposed to interact in the considered class of problems and the wave propagation may change drastically between various subdomains, because the wavelengths are different. Moreover, in poroelastic media there are three types of waves that propagate with different velocities: two compressional waves and a shear wave. The propagation velocities may also strongly depend on frequency since porous materials are dispersive. Thus, generally speaking, different finite element meshes are required for various subdomains with sufficient densities to satisfy a common requirement of several elements per wavelength, and this should be done for the shortest waves and so for the highest frequency of interest. It is obvious though, that the required size of elements will vary drastically for subdomains of various media and for some, let us say, "longer-wavelegth" subdomains, the elements in the vicinity of the interfaces with "shorter-wavelegth" subdomains may need to be significantly smaller than the required size, in order to maintain the geometrical quality of the mesh. Another important issue is the approximation order. Generally speaking, for poroelastic subdomains, which require rather dense meshes, the second-order approximation is usually much more advantageous than linear shape functions possible in case of very dense discretizations. For subdomains of air coarse meshing and linear shape functions can be used, whereas for the elastic and (usually thin) piezoelectric subdomains the second-order (quadratic Lagrange) polynomials should be preferred as shape functions for all the component-fields of displacement, as well as for the scalar field of electric potential. The second-order approximation of electric potential is quite important for accurate estimation of voltage amplitudes used in active control since the first-order interpolation would result in a linear through-thickness variation of the electric potential and that would neglect the induced potential and the electromechanical coupling would be partial [6].

3. Biot's theory of poroelasticity

The Biot's theory of poroelasticity [7, 1, 2] provides a biphasic model of porous media: the so-called solid phase is used to describe the behavior of the ("smeared") elastic skeleton whereas the fluid phase pertains to the fluid in the pores. Both phases are two coupled homogeneous continua. The most frequently-used version of poroelasticity assumes besides that both phases are isotropic. Moreover, the fluid is modelled as inviscid, though viscous forces, are taken into account but only when modeling interaction between the fluid and the solid frame.

In the classical formulation [7, 1, 8, 2] a state of poroelastic medium is described by the displacements of solid, $\mathbf{u} = \{u_i\}$, and fluid phase, $\mathbf{U} = \{U_i\}$. The Biot's equations for a local dynamic equilibrium of poroelastic material link partial stress tensors associated with the skeleton particle (σ^{s}_{ij}) and the macroscopic fluid particle (σ^{f}_{ij}) with the solid and fluid macroscopic

displacements. In the case of harmonic oscillations (with angular frequency ω) these equations read

$$\sigma^{\mathrm{s}}_{ij|j} + \omega^2 \tilde{\varrho}_{\mathrm{ss}}\, u_i + \omega^2 \tilde{\varrho}_{\mathrm{sf}}\, U_i = 0 \,,$$
$$\sigma^{\mathrm{f}}_{ij|j} + \omega^2 \tilde{\varrho}_{\mathrm{ff}}\, U_i + \omega^2 \tilde{\varrho}_{\mathrm{sf}}\, u_i = 0 \,, \tag{2}$$

where the frequency-dependent effective densities, $\tilde{\varrho}_{\mathrm{ss}}$, $\tilde{\varrho}_{\mathrm{sf}}$, and $\tilde{\varrho}_{\mathrm{ff}}$, are introduced. These densities are responsible not only for the inertia of solid or fluid phase particles but also for the combined inertial and viscous coupling (interaction) of both phases. They depend on the viscous drag coefficient, $\tilde{b}$, and the normal effective densities, ϱ_{ss}, ϱ_{ff}, ϱ_{sf}. The latter quantities in turn depend on the porosity, ϕ, the tortuosity of pores, α_∞, the density of the material of skeleton, ϱ_{s}, and the density of saturating fluid, ϱ_{f}. The adequate formulas may be found in [1, 2].

The partial solid and fluid stress tensors are linearly related to the partial strain tensors prevailing in the skeleton and the interstitial fluid. This is given by the following linear and isotropic constitutive equations of the Biot's theory of poroelasticity:

$$\sigma^{\mathrm{s}}_{ij} = \mu_{\mathrm{s}}\left(u_{i|j} + u_{j|i}\right) + \left(\tilde{\lambda}_{\mathrm{s}}\, u_{k|k} + \tilde{\lambda}_{\mathrm{sf}}\, U_{k|k}\right)\delta_{ij} \,,$$
$$\sigma^{\mathrm{f}}_{ij} = \left(\tilde{\lambda}_{\mathrm{f}}\, U_{k|k} + \tilde{\lambda}_{\mathrm{sf}}\, u_{k|k}\right)\delta_{ij} \,. \tag{3}$$

Four material constants are involved here, namely μ_{s}, $\tilde{\lambda}_{\mathrm{s}}$, $\tilde{\lambda}_{\mathrm{f}}$, and $\tilde{\lambda}_{\mathrm{sf}}$. The first two of them resemble the two Lamé coefficients of isotropic elasticity. Moreover, μ_{s} is the shear modulus of the poroelastic material and consequently the shear modulus of the frame since the fluid does not contribute to the shear restoring force. The three dilatational constants, $\tilde{\lambda}_{\mathrm{s}}$, $\tilde{\lambda}_{\mathrm{f}}$ and $\tilde{\lambda}_{\mathrm{sf}}$ are frequency-dependent and are functions of K_{b}, K_{s}, and $\tilde{K}_{\mathrm{f}}$ ($\tilde{\lambda}_{\mathrm{s}}$ depends also on μ_{s}), where: K_{b} is the bulk modulus of the frame at constant pressure in the fluid, K_{s} is the bulk modulus of the elastic solid from which the frame is made, and $\tilde{K}_{\mathrm{f}}$ is the bulk modulus of the fluid in porous medium. The adequate formulas to compute the poroelastic material constants can be found in [1, 2]. Finally, the total stress tensor of poroelastic medium is defined as a simple sum of the partial, i.e. phasic, stress tensors, whereas the total displacement vector sums up porosity-dependent contributions of the displacements of both phases:

$$\sigma^{\mathrm{t}}_{ij} = \sigma^{\mathrm{s}}_{ij} + \sigma^{\mathrm{f}}_{ij} \,, \qquad u^{\mathrm{t}}_i = (1 - \phi)\, u_i + \phi\, U_i \,. \tag{4}$$

The equations of equilibrium (2) together with the constitutive relations (3) form the displacement formulation of linear, isotropic poroelasticity for harmonic oscillations. Notice that the first equations from both pairs refer to the solid phase whereas the second ones to the fluid phase. Nevertheless, both phases are strongly coupled by the viscous-inertial coupling coefficient, $\tilde{\varrho}_{\mathrm{sf}}$, and the constitutive coupling constant, $\tilde{\lambda}_{\mathrm{sf}}$. In this classical formulation the unknown fields are the solid and fluid phase displacements, which means 6 degrees of freedom in every node of a three-dimensional model.

The fluid phase stress tensor can be expressed as

$$\sigma^{\mathrm{f}}_{ij} = -\phi\, p\, \delta_{ij} \,, \tag{5}$$

where p is the pressure of fluid in the pores (it should not be mistaken for the pressure of fluid phase which equals ϕp). By using this relation for the time-harmonic version of Biot's poroelasticity, the fluid phase displacements can be expressed as functions of the pressure in the pores, and thus eliminated from the equations (replaced by p); such derivation can be found in [19]. This results in the mixed displacement–pressure formulation [4, 9, 2] where the dependent variables are the three solid phase displacements and the pore-fluid pressure. Therefore, three-dimensional models have now only 4 degrees of freedom in a node.

4. Weak forms of poroelasticity, elasticity, piezoelectricity, and acoustics

4.1. Weak form for the mixed formulation of poroelasticity

Let Ω_p be a domain of poroelastic material and Γ_p its boundary with n_i being the components of the unit vector normal to the boundary and pointing outside the domain. The harmonic poroelasticity problem can be described in this domain by the mixed formulation which uses as dependent variables the solid phase displacements, u_i, and pore-fluid pressure, p. The corresponding weak form [3, 2] reads as follows (for every admissible δu_i and δp)

$$
\begin{aligned}
\mathcal{WF}_\mathrm{p} = & -\int_{\Omega_\mathrm{p}} \sigma_{ij}^\mathrm{ss}\, \delta u_{i|j} + \int_{\Omega_\mathrm{p}} \omega^2\, \tilde{\varrho}\, u_i\, \delta u_i - \int_{\Omega_\mathrm{p}} \frac{\phi^2}{\omega^2 \tilde{\varrho}_\mathrm{ff}}\, p_{|i}\, \delta p_{|i} \\
& + \int_{\Omega_\mathrm{p}} \frac{\phi^2}{\tilde{\lambda}_\mathrm{f}}\, p\, \delta p + \int_{\Omega_\mathrm{p}} \phi\left(1 + \frac{\tilde{\varrho}_\mathrm{sf}}{\tilde{\varrho}_\mathrm{ff}}\right) \delta(p_{|i}\, u_i) \quad (6) \\
& + \int_{\Omega_\mathrm{p}} \phi\left(1 + \frac{\tilde{\lambda}_\mathrm{sf}}{\tilde{\lambda}_\mathrm{f}}\right) \delta(p\, u_{i|i}) + \mathcal{BI}_\mathrm{p}\,,
\end{aligned}
$$

where

$$
\sigma_{ij}^\mathrm{ss} = \mu_\mathrm{s}\,(u_{i|j} + u_{j|i}) + \left(\tilde{\lambda}_\mathrm{s} - \frac{\tilde{\lambda}_\mathrm{sf}^2}{\tilde{\lambda}_\mathrm{f}}\right) u_{k|k}\, \delta_{ij} \text{ and } \tilde{\varrho} = \tilde{\varrho}_\mathrm{ss} - \frac{\tilde{\varrho}_\mathrm{sf}^2}{\tilde{\varrho}_\mathrm{ff}}\,,
\tag{7}
$$

$\mathcal{BI}_\mathrm{p}$ is the boundary integral

$$
\mathcal{BI}_\mathrm{p} = \int_{\Gamma_\mathrm{p}} \sigma_{ij}^\mathrm{t}\, n_j\, \delta u_i + \int_{\Gamma_\mathrm{p}} \phi\,(U_i - u_i)\, n_i\, \delta p\,,
\tag{8}
$$

whereas δu_i and δp are test (or weighting) functions, that is, arbitrary yet admissible virtual displacements and pressure. Below, the two most relevant boundary conditions of poroelastic medium are discussed [9, 3, 2].

Relevant boundary conditions. Two types of boundary conditions will be discussed here, namely: an imposed displacement field and an imposed pressure field.

A displacement field, $\hat{u}_i$, applied on a boundary of a poroelastic medium describes, for example, a case of a piston in motion acting on the surface of the medium. Here, it is assumed that the solid skeleton is fixed to the surface of piston while the fluid obviously cannot penetrate into the piston. Therefore, on Γ_p^u:

$$
u_i = \hat{u}_i\,, \qquad (U_i - u_i)\, n_i = 0\,.
\tag{9}
$$

The first condition expresses the continuity between the imposed displacement vector and the solid phase displacement vector. The second equation expresses the continuity of between the normal displacements of the solid phase and the fluid phase. Using these conditions and the fact that the variations of the known solid displacements are zero ($\delta u_i = 0$) the boundary integral reduces to zero:

$$
\mathcal{BI}_\mathrm{p} = 0 \text{ on } \Gamma_\mathrm{p}^u\,.
\tag{10}
$$

A harmonic pressure field of amplitude $\hat{p}$ is imposed on the boundary of a poroelastic domain which means that it affects at the same time the fluid in the pores and the solid skeleton. Therefore, the following boundary conditions must be met on Γ_p^p:

$$
p = \hat{p}\,, \qquad \sigma_{ij}^\mathrm{t}\, n_j = -\hat{p}\, n_i\,.
\tag{11}
$$

The first condition is of Dirichlet type and must be applied explicitly. It describes the continuity of pressure in the fluid. It means

also that the pressure variation is zero ($\delta p = 0$) at the boundary. The second condition expresses the continuity of the total normal stress. All this, when used for Equation (8), leads to the following boundary integral

$$
\mathcal{BI}_\mathrm{p} = \int_{\Gamma_\mathrm{p}} \sigma_{ij}^\mathrm{t}\, n_j\, \delta u_i = -\int_{\Gamma_\mathrm{p}^p} \hat{p}\, n_i\, \delta u_i\,.
\tag{12}
$$

4.2. Weak form for an elastic solid

Let Ω_e be an elastic solid domain with mass density ϱ_e and boundary Γ_e, and n_i^e the components of unit vector normal to the boundary and pointing outside the domain. Assuming zero body forces and the case of harmonic oscillations the weak variational form of the problem of elasticity expressing the principle of virtual work reads [19] (for every admissible δu_i^e)

$$
\mathcal{WF}_\mathrm{e} = -\int_{\Omega_\mathrm{e}} \sigma_{ij}^\mathrm{e}\, \delta u_{i|j}^\mathrm{e} + \int_{\Omega_\mathrm{e}} \omega^2\, \varrho_\mathrm{e}\, u_i^\mathrm{e}\, \delta u_i^\mathrm{e} + \int_{\Gamma_\mathrm{e}} \sigma_{ij}^\mathrm{e}\, n_j^\mathrm{e}\, \delta u_i^\mathrm{e}\,,
\tag{13}
$$

where δu_i^e is the arbitral yet admissible variation of displacements; the elastic stress tensor $\sigma_{ij}^\mathrm{e} = \sigma_{ij}^\mathrm{e}(\mathbf{u}^\mathrm{e})$ substitutes here a linear function of elastic displacements $\mathbf{u}^\mathrm{e} = \{u_i^\mathrm{e}\}$. In the case of the linear isotropic elasticity it can be expressed as follows

$$
\sigma_{ij}^\mathrm{e} = \mu_\mathrm{e}\,(u_{i|j}^\mathrm{e} + u_{j|i}^\mathrm{e}) + \lambda_\mathrm{e}\, u_{k|k}^\mathrm{e}\, \delta_{ij}\,,
\tag{14}
$$

where the well-known Lamé coefficients, the shear modulus μ_e and the dilatational constant λ_e, appear.

Boundary conditions. For the sake of brevity, only von Neumann and Dirichlet boundary conditions for an elastic solid will be discussed. The Neumann (or natural) boundary conditions describe the case when forces $\hat{t}_i^\mathrm{e}$ are applied on a boundary, that is

$$
\sigma_{ij}^\mathrm{e}\, n_j^\mathrm{e} = \hat{t}_i^\mathrm{e} \text{ on } \Gamma_\mathrm{e}^t\,,
\tag{15}
$$

whereas the displacements, $\hat{u}_i^\mathrm{e}$, are prescribed by the Dirichlet (or essential) boundary conditions

$$
u_i^\mathrm{e} = \hat{u}_i^\mathrm{e} \text{ on } \Gamma_\mathrm{e}^u\,.
\tag{16}
$$

According to these conditions the boundary is divided into two (directionally disjoint) parts, i.e. $\Gamma_\mathrm{e} = \Gamma_\mathrm{e}^t \cup \Gamma_\mathrm{e}^u$. There is an essential difference between the two kinds of conditions. The displacement constraints form the kinematic requirements for the trial functions, u_i^e, while the imposed forces appear in the weak form; thus, the boundary integral, that is the last of the integrals of Eq. (13), equals

$$
\mathcal{BI}_\mathrm{e} = \int_{\Gamma_\mathrm{e}} \sigma_{ij}^\mathrm{e}\, n_j^\mathrm{e}\, \delta u_i^\mathrm{e} = \int_{\Gamma_\mathrm{e}^t} \hat{t}_i^\mathrm{e}\, \delta u_i^\mathrm{e}\,.
\tag{17}
$$

Here, the property $\delta u_i^\mathrm{e} = 0$ on Γ_e^u has been used.

4.3. Weak form of piezoelectricity

The theory of piezoelectricity is extensively discussed, for example, in [13, 15]. More or less brief recapitulations of the linear theory of piezoelectricity may be found also in many papers and books on active vibration control and piezoelectric actuators and sensors (e.g., [10, 16, 17]). A very good survey of the advances and trends in finite element modeling of piezoelectricity was presented by Benjeddou [6]. In this paper the basic theoretical considerations and equations of linear piezoelectricity as well as the variational piezoelectric equations are also given.

Piezoelectric elements (actuators and sensors) of the proposed active composites, liners and panels are to be modeled using the linear theory. It is adequate enough and, moreover, it is a very accurate model when comparing it to some frequently used approximations (as a matter of fact, the so-called thermal analogy

approach is usually an acceptable approximation when modeling piezo-actuators). Here, a variational form of linear piezoelectricity will be presented as being the most used one for piezoelectric finite element formulations. This form should be regarded as the sum of the conventional principle of virtual mechanical displacements and the principle of virtual electric potential.

Let Ω_pz be a domain of piezoelectric material, ϱ_pz its mass density, and Γ_pz its boundary. The unit boundary-normal vector, n_i^pz, points outside the domain. The dependent variables of piezoelectric medium are the mechanical displacements, u_i^pz, and electric potential, V^pz. The case of harmonic oscillations (with the angular frequency ω) with no mechanical body forces and electric body charge is considered. Then, for arbitrary yet admissible virtual displacements, δu_i^pz, and virtual electric potential, δV^pz, the variational formulation of the piezoelectricity problem can be given as

$$\mathcal{WF}_\text{pz} = -\int\limits_{\Omega_\text{pz}} \sigma_{ij}^\text{pz}\, \delta u_{i|j}^\text{pz} + \int\limits_{\Omega_\text{pz}} \omega^2 \varrho_\text{pz}\, u_i^\text{pz}\, \delta u_i^\text{pz} + \int\limits_{\Gamma_\text{pz}} \sigma_{ij}^\text{pz}\, n_j^\text{pz}\, \delta u_i^\text{pz}$$
$$-\int\limits_{\Omega_\text{pz}} D_i^\text{pz}\, \delta V_{|i}^\text{pz} + \int\limits_{\Gamma_\text{pz}} D_i^\text{pz}\, n_i^\text{pz}\, \delta V^\text{pz}, \tag{18}$$

where $\sigma_{ij}^\text{pz} = \sigma_{ij}^\text{pz}(\mathbf{u}^\text{pz}, V^\text{pz})$ and $D_i^\text{pz} = D_i^\text{pz}(\mathbf{u}^\text{pz}, V^\text{pz})$ are expressions of mechanical displacements and electric potential. Obviously, from the physical point of view they represent the mechanical stress tensor and the electric displacement vector, respectively. As a matter of fact, these expressions are the so-called *stress-charge form* of the constitutive relations of piezoelectricity – they are given below for the case of linear anisotropic piezoelectricity:

$$\sigma_{ij}^\text{pz} = C_{ijkl}^\text{pz}\, \frac{u_{k|l}^\text{pz} + u_{l|k}^\text{pz}}{2} - e_{kij}^\text{pz}\, V_{|k}^\text{pz},$$
$$D_i^\text{pz} = e_{ikl}^\text{pz}\, \frac{u_{k|l}^\text{pz} + u_{l|k}^\text{pz}}{2} + \epsilon_{ik}^\text{pz}\, V_{|k}^\text{pz}. \tag{19}$$

Here, C_{ijkl}^pz, e_{ikl}^pz, and ϵ_{ik}^pz denote (the components of) the fourth-order tensor of elastic material constants, the third-order tensor of piezoelectric material constants, and the second-order tensor of dielectric material constants, respectively. These three tensors of material constants characterize completely any piezoelectric material, i.e., its elastic, piezoelectric, and dielectric properties. Only one of these tensors is responsible for the piezoelectric effects. Therefore, piezoelectricity can be viewed as a multiphysics problem where in one domain of a piezoelectric medium the problems of elasticity and electricity are coupled by the piezoelectric material constants present in (additional) coupling terms in the constitutive relations. One should notice that the (linear) kinematic relations, $\varepsilon_{ij}^\text{pz} = \frac{u_{k|l}^\text{pz} + u_{k|l}^\text{pz}}{2}$, linking mechanical strain ($\varepsilon_{ij}^\text{pz}$) and displacements ($u_i^\text{pz}$), and the Maxwell's law for electrostatics, $E_i^\text{pz} = -V_{|i}^\text{pz}$, relating the electric field (E_i^pz) with its potential (V^pz), have been explicitly used in Eqs. (19).

Boundary conditions. In piezoelectricity the boundary conditions are divided into two groups – there are mechanical conditions (referring to the elasticity problem) and electrical conditions (referring to the electricity). Consequently, the boundary of piezoelectric domain can be subdivided as follows:

$$\Gamma_\text{pz} = \Gamma_\text{pz}^t \cup \Gamma_\text{pz}^u \quad \text{and} \quad \Gamma_\text{pz} = \Gamma_\text{pz}^Q \cup \Gamma_\text{pz}^V. \tag{20}$$

The parts belonging to the same group of subdivision are disjoint and both subdivisions are completely independent. Here, Γ_pz^t and Γ_pz^Q pertain to the Neumann conditions for surface-applied mechanical forces and electric charge, respectively, while Γ_pz^u and

Γ_pz^V refer to the Dirichlet conditions on imposed mechanical displacements and electric potential, respectively. The third possibility of Robin boundary condition is skipped; however, it would involve another parts – one in the mechanical and one in the electric subdivision of the boundary.

First, consider the mechanical boundary conditions. The forces, $\hat{t}_i^\text{pz}$, applied to a boundary are expressed by the Neumann (or natural) condition

$$\sigma_{ij}^\text{pz}\, n_j^\text{pz} = \hat{t}_i^\text{pz} \text{ on } \Gamma_\text{pz}^t, \tag{21}$$

whereas the imposed displacements, $\hat{u}_i^\text{pz}$, will appear in the Dirichlet (i.e., essential) boundary condition

$$u_i^\text{pz} = \hat{u}_i^\text{pz} \text{ on } \Gamma_\text{pz}^u. \tag{22}$$

The Dirichlet condition must be *a priori* explicitly met by the trial functions while the Neumann condition (21) is used for the mechanical boundary integral, that is, the third term in Equation (18), which equals

$$\mathcal{BI}_\text{pz}^\text{mech} = \int\limits_{\Gamma_\text{pz}} \sigma_{ij}^\text{pz}\, n_j^\text{pz}\, \delta u_i^\text{pz} = \int\limits_{\Gamma_\text{pz}^t} \hat{t}_i^\text{pz}\, \delta u_i^\text{pz}, \tag{23}$$

since $\delta u_i^\text{pz} = 0$ on Γ_pz^u.

The electric boundary condition of the Neumann kind serves for a surface electric charge $\hat{Q}^\text{pz}$ applied on a boundary

$$-D_i^\text{pz}\, n_i^\text{pz} = \hat{Q}^\text{pz} \text{ on } \Gamma_\text{pz}^Q, \tag{24}$$

whereas the Dirichlet condition allows to prescribe the electric potential $\hat{V}^\text{pz}$ on a boundary

$$V^\text{pz} = \hat{V}^\text{pz} \text{ on } \Gamma_\text{pz}^V. \tag{25}$$

The electric boundary integral, that is, the last term in Equation (18) equals

$$\mathcal{BI}_\text{pz}^\text{elec} = -\int\limits_{\Gamma_\text{pz}} D_i^\text{pz}\, n_i^\text{pz}\, \delta V^\text{pz} = \int\limits_{\Gamma_\text{pz}^Q} \hat{Q}^\text{pz}\, \delta V^\text{pz}. \tag{26}$$

Here, the Neumann condition for electric charge (24) has been used together with the condition for voltage variation, $\delta V^\text{pz} = 0$ on Γ_pz^V.

By summing up the mechanical and electrical boundary integrals (23) and (26), the following total mechanical-electric boundary integral results:

$$\mathcal{BI}_\text{pz} = \mathcal{BI}_\text{pz}^\text{mech} + \mathcal{BI}_\text{pz}^\text{elec} = \int\limits_{\Gamma_\text{pz}^t} \hat{t}_i^\text{pz}\, \delta u_i^\text{pz} + \int\limits_{\Gamma_\text{pz}^Q} \hat{Q}^\text{pz}\, \delta V^\text{pz}. \tag{27}$$

4.4. Weak form for an acoustic medium

Let Ω_a be an acoustic medium domain, that is a domain of inviscid fluid, and Γ_a its boundary with n_i^a being the components of unit normal vector pointing outside the domain. The dependent variable of acoustical medium is the acoustic pressure, p^a. Finite element methods for time-harmonic acoustics are reviewed in [12, 18]. For harmonic motion with the angular frequency ω, the following weak form should be used:

$$\mathcal{WF}_\text{a} = -\int\limits_{\Omega_\text{a}} \frac{1}{\omega^2 \varrho_\text{a}}\, p_{|i}^\text{a}\, \delta p_{|i}^\text{a} + \int\limits_{\Omega_\text{a}} \frac{1}{\varrho_\text{a}\, c_\text{a}^2}\, p^\text{a} \delta p^\text{a} + \int\limits_{\Gamma_\text{a}} \frac{1}{\omega^2 \varrho_\text{a}}\, p_{|i}^\text{a}\, n_i^\text{a}\, \delta p^\text{a},$$
$$\tag{28}$$

where ϱ_a is the acoustic medium mass density and c_a is the speed of sound. Knowing the acoustic pressure one can always determine the (complex amplitudes of) displacements, velocities and accelerations of fluid particle using the following formulas:

$$u_i^a = \frac{1}{\omega^2 \varrho_a}\, p_{|i}^a\,, \quad v_i^a = j\,\omega\, u_i^a = -\frac{1}{j\,\omega\, \varrho_a}\, p_{|i}^a\,,$$

$$a_i^a = -\omega^2\, u_i^a = -\frac{1}{\varrho_a}\, p_{|i}^a\,. \tag{29}$$

Boundary conditions: When a value of acoustic pressure, $\hat{p}^a$, is prescribed, the Dirichlet boundary condition simply states that

$$p^a = \hat{p}^a \text{ on } \Gamma_a^p\,. \tag{30}$$

When a rigid piston of known acceleration, $\hat{a}_i^a$, is imposed on a boundary – in the harmonic case $\hat{a}_i^a = -\omega^2\, \hat{u}_i^a$, where $\hat{u}_i^a$ is the (complex) amplitude of displacements – the following Neumann condition is used

$$\frac{1}{\omega^2 \varrho_a}\, p_{|i}^a = \hat{u}_i^a \text{ on } \Gamma_a^u\,. \tag{31}$$

Using this condition and the condition for pressure variation, $\delta p^a = 0$ on Γ_a^p, the boundary integral, that is, the last term in Equation (28), can be written as follows:

$$\mathcal{BI}_a = \int_{\Gamma_a} \frac{1}{\omega^2 \varrho_a}\, p_{|i}^a\, n_i^a\, \delta p^a = \int_{\Gamma_a^u} \hat{u}_i^a\, n_i^a\, \delta p^a\,. \tag{32}$$

The acoustic impedance can be prescribed at a boundary by the Robin's type of boundary condition, which is a linear combination of the Dirichlet's and Neumann's kinds. Finally, the so-called non-reflecting boundary conditions (NRBC) [11] often play an important role, because they ensure that no (or little) spurious wave reflection occurs from the boundary.

5. Numerical example

5.1. Active sandwich panel

A few results of numerical analysis carried out for a disk of sandwich panel with poroelastic core, and a thin PZT-ceramic patch fixed to one of its faceplates, will be presented below. Figure 1 shows a lateral view of such panel fitted into a rigid-walled air waveguide, so it can smoothly slide along. The total thickness of panel (without PZT-patch) is 20 mm and its diameter is 100 mm. The PZT-patch is 0.3 mm thick; it is also circular in shape and it is fixed in the centre of the circular faceplate of panel. Therefore, the whole configuration of the panel in air waveguide is perfectly symmetric relative to its axis, and thus, a two-dimensional axially-symmetric modelling of the representative domain of panel with as adjacent fragment of air waveguide (the rectangle ABCD shown in Fig. 1) is fully justified.

A plane, time-harmonic, acoustic wave propagates in the air waveguide onto the panel's surface. It is partially reflected, partially absorbed, and partially transmitted through the panel. The acoustic transmission through the panel was analysed for the passive and active cases. The feasibility of active approach – involving complex two-dimensional deformations – can be studied, provided that the finite-element model is reliable: as a matter of fact, various results of acoustic transmission (some of which are going to be presented below) were also utilized to validate the convergence of finite element solutions.

5.2. Results of the passive behaviour

Several finite element analyses were carried out to test passive behaviour of sandwich panel. Figure 3 presents the sound pressure level calculated for purely passive panel at point D

(60 mm from the lower surface of panel, see Fig. 1) for harmonic acoustic excitation with the amplitude of 1 Pa as described in the previous Section. Four results are plotted in the form of SPL curves. Three of them, namely, (a), (b) and (c), were obtained for two-dimensional, axially-symmetric, finite-element models using coarse or dense meshes, and linear or quadratic approximations in poroelastic domain. The elastic faceplates were always approximated using the second-order shape functions. The fourth curve (d) is a result of one-dimensional analytical solution. Since no piezoelectric patch was present in the finite element models the one-dimensional modelling is fully appropriate under the circumstances described above (that is, the applied boundary conditions and uniformly distributed acoustic pressure excitation), and thus, the analytical solution is exact for such configuration of purely passive panel. From Fig. 3 it can be seen that the results for the proposed two-dimensional finite-element models are very accurate even for the coarsest of meshes with linear approximation in poroelastic domain (notice that some discrepancies visible for this model in the range above 3 kHz are for SPL below 10 dB). Thus, the general conclusion is that all the considered models are in fact valid for passive analyses, so that the very economical coarse-mesh model with linear approximation in poroelastic domain may be used. It will be demonstrated, however, that it is not true in the case of the active approach.
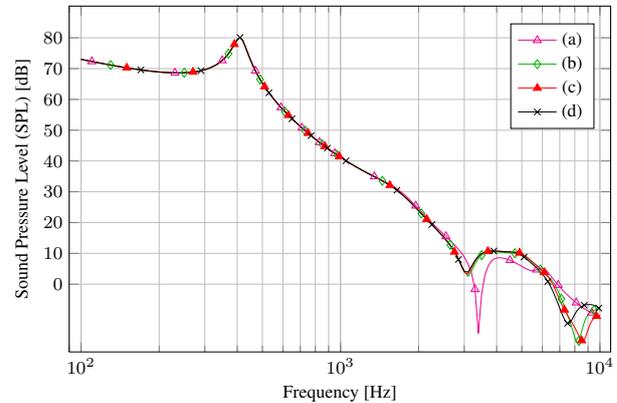

Figure 3: The sound pressure level (SPL) at point D for: (a) the 2D axial model with the coarse mesh and a linear approximation in the poroelastic domain, (b) the 2D axial model with the dense mesh and a linear approximation in the poroelastic domain, (c) the 2D axial model with the coarse mesh and a quadratic approximation in the poroelastic domain, (d) the analytical solution.

5.3. Feasibility and convergence tests of the active approach

The results of passive analysis presented in Fig. 3 show that the panel exhibit a resonance behaviour at the frequency slightly above 400 Hz. Around this frequency the acoustic insulation is very poor, and in general, it is not very effective at lower frequencies. To alleviate this problem the active approach should be used.
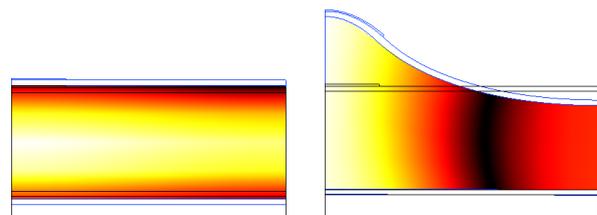

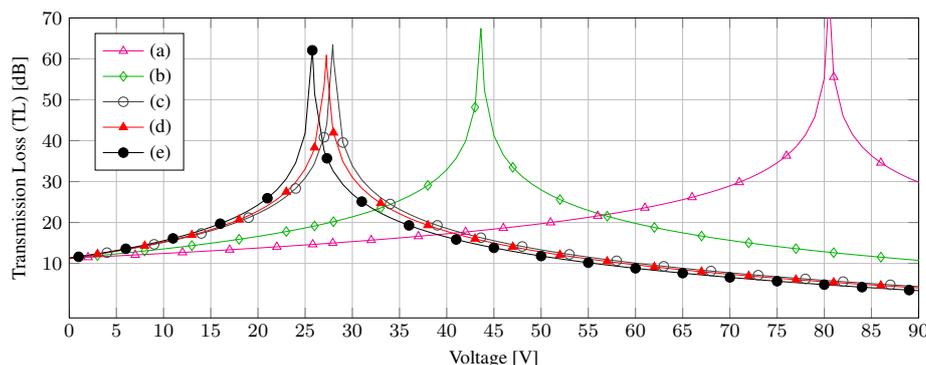Figure 4: Passive and active behaviour of panel at 400 Hz

Figure 5: Some h- and p-convergence solutions for active improvement of transmission loss (TL) at 400 Hz obtained for: (a) a coarse mesh with linear approximation in poroelastic domain (364 DOFs), (b) a dense mesh with linear approximation in poroelastic domain (2738 DOFs), (c) a very dense mesh with linear approximation in poroelastic domain (10040 DOFs), (d) a coarse mesh with quadratic approximation in poroelastic domain (551 DOFs), (e) a very dense mesh with quadratic approximation everywhere (39305 DOFs).

The passive and active behaviour of panel at 400 Hz is compared in Fig. 4. In the passive case, the excitation is by a plane harmonic wave with the pressure amplitude of 1 Pa impinging the upper faceplate of panel. In the active case, apart from the acoustic excitation, a harmonic voltage signal of the same frequency of 400 Hz is applied to the electrodes of the piezo-patch actuator. The actuator is in that way harmonically expanded and contracted, which induces some bending deformation of the upper faceplate, affecting the vibrations of the panel. It is possible to choose the amplitude (and phase) of the signal necessary to better attenuate the acoustic wave transmitted through the panel. To this end, the acoustic pressure below the panel should be observed. It should be noticed that in the passive case the transmitted wave is plane, yet in the case of the active approach it may not be plane in the vicinity of the lower faceplate because of the additional, non-uniform, electric excitation induced on the upper faceplate. Thus, in the active case, the vibrations of the lower faceplate may not be planar, depending on the frequency of excitations, the thickness and material properties of poroelastic core, etc. Nevertheless, at some distance from the lower faceplate the transmitted acoustic wave is plane. This is certainly on the line CD situated across the waveguide, 60 mm from the lower faceplate. Therefore, the acoustic pressure of the transmitted wave will be observed at point D – which should be in practice equal to the acoustic pressure at any other point on the line CD – or, alternatively, a measure of the acoustic pressure defined as an integral of the pressure along the line CD may be used. As a matter of fact, one should notice that this approach complies actually with the experimental practice: during the measurements the microphones are situated at some distance from the sample. The vibration shapes of panel, shown in Fig. 4 for the passive and active states, are scaled by the same scaling factor. It can be observed that the maximal vibrations in the active case are several times bigger than in the passive case. Nevertheless, they are still very small and fully comply with the linear regime. The necessary voltage amplitude was estimated as app. 26 V. Since the piezo-patch actuators are fixed to the upper faceplate the phase shift was negligible, and the necessary voltage was found by some parametric analyses involving sweeping of voltage amplitude, after some convergence tests – discussed below – had been carried out. Alternatively, it can be found using the method described in the next Section, involving two harmonic analysis.

Figure 5 presents some of the p- and h-convergence tests of the active approach performed for various finite element models. The acoustic transmission reduction was computed for the mutual, 400 Hz-harmonic excitations by the acoustic wave with the amplitude of 1 Pa, and the active electrical signal with the amplitude swept from 0 V to 90 V. The curves (a), (b) and (c) from

Fig. 5 present the h-convergence of the active solution – when the mesh density is increased and the approximation remains linear, whereas the curves (a) and (d), as well as the curves (c) and (e) present two p-convergence solutions – when the approximation order is increased, from linear to quadratic, and the mesh density remains unchanged, coarse or very dense, respectively in these two cases. It is remarkable that all the curves start from the same point at 0 V, which confirms that for the passive case all the models give the same results. However, when the voltage is increased, the coarse and dense-mesh models with linear approximation in poroelastic domain give solutions – the curves (a) and (b) – which are significantly different from the results obtained with the very dense-mesh models. Thus, it can be stated that the models with linear shape functions are not appropriate for the active analyses if their meshes are not extremely dense; they give very exaggerated estimations for the proper voltage amplitudes of active reduction signals. On the other hand, the curves (c) and (d), obtained for the *very dense* mesh with linear approximation in poroelastic domain, and for the coarse mesh with *quadratic* approximation, respectively, are very close to the curve (e) obtained when the accurate model with the very dense mesh and quadratic approximation was used. Eventually, a conclusion must be drawn that the model with the coarse mesh but with quadratic approximation in poroelastic domain, gives very good results, being at the same time very economical (only 551 DOF).

5.4. *Frequency analyses and a parametric survey for the active approach*

Figure 6 presents parametric sweeps performed in order to estimate optimal voltage amplitudes for the active reduction of vibroacoustic transmission at different frequencies. For each of several computational frequencies from 250 Hz to 800 Hz, the voltage amplitude of active signal was swept to find the minimum of the sound pressure level computed at point D which meant also the maximum of the transmission loss. The optimization of the phase of the signal was neglected since the piezo-patch actuator affects directly the upper faceplate, where the acoustic excitation is also directly applied, and the elastic faceplate is assumed lossless. The results shown in Fig. 6 clearly confirm that at lower frequencies higher voltages for active signals are necessary.

The right-hand side graph in Fig. 6 summarizes the results of optimal voltage amplitudes found for the PZT-patch actuator of radius 10 mm. These results were also obtained by the following calculation procedure. First, a pressure measure, for example, the acoustic pressure, at the distance of 60 mm from the lower faceplate is computed for the harmonic excitation by the plane acoustic wave with the amplitude of 1 Pa; let the result be termed
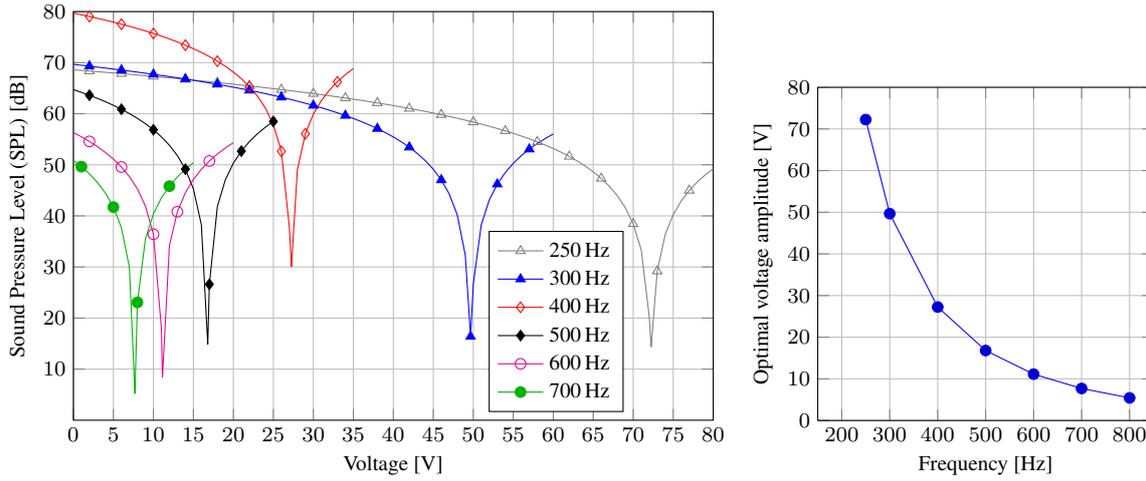
Figure 6: Optimal voltage amplitudes for the active reduction of vibroacoustic transmission at different frequencies
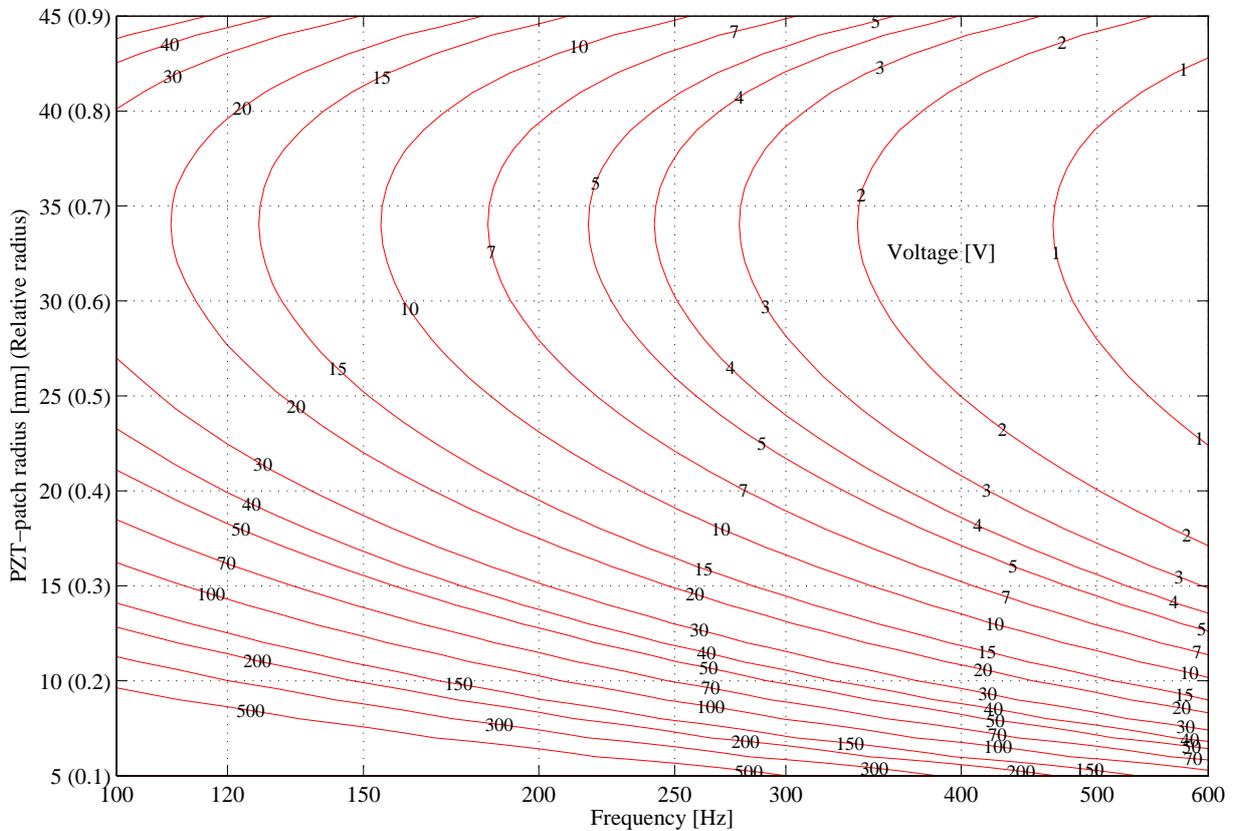

Figure 7: Optimal voltage amplitudes for the active reduction signals

as α [Pa]. Then, the pressure measure is calculated for only electrical excitation with the voltage amplitude of 1 V; let the result be termed as β [Pa]. Since the system is linear, the pressure response at 60 mm for simultaneous, acoustic and electric excitations can be computed as follows

$$p^{\mathrm{a}}_{\mathrm{at}\,60\,\mathrm{mm}} = \frac{\alpha}{1\,\mathrm{Pa}}\,\hat{p} + \frac{\beta}{1\,\mathrm{V}}\,\hat{U}, \tag{33}$$

where $\hat{p}$ [Pa] and $\hat{U}$ [V] are the amplitudes of the acoustical and electrical excitations, respectively. Now, from the requirement that $p^{\mathrm{a}}_{\mathrm{at}\,60\,\mathrm{mm}} \approx 0$ Pa, the necessary amplitude for the active sig-

nal may be estimated as:

$$\hat{U} = -\frac{\alpha}{\beta}\frac{\mathrm{V}}{\mathrm{Pa}}\,\hat{p} = -\frac{\alpha}{\beta}\,\mathrm{V}. \tag{34}$$

Here, it has been assumed that the amplitude of acoustic excitation is $\hat{p} = 1$ Pa. Notice that α, β, and $\hat{U}$ are in general complex amplitudes. This procedure was extensively used for a parametric survey where the optimal voltage amplitudes for active signals were estimated at different frequencies for different sizes of the piezoelectric actuator. The radii of the PZT-patch were taken from 5 mm to 45 mm, whereas the computational frequencies were from the range of 100 Hz to 600 Hz. The results are

given in Fig. 7, where it can be observed that the optimal radius of PZT-patch is approximately 35 mm: the smallest voltage amplitudes are required in the whole considered frequency range for such PZT actuator. It means that when the radius is bigger or smaller than 35 mm the optimal voltage amplitude increases. Nevertheless, quite a good performance has a PZT-patch with the radius of only 16 mm, for which – even at the lowest considered frequency of 100 Hz – the required voltage amplitudes for active signal are not bigger than several dozens of volts.

6. Conclusions

A fully-coupled finite-element modelling of active-passive systems for vibroacoustic attenuation, involving poroelastic, piezoelectric, and elastic materials, as well as "acoustic" (inviscid) fluids has been discussed. The proposed multiphysics system is suitable for numerical analyses of active sandwich panels with poroelastic core and allows for advanced parametric studies.

Acknowledgements

References

[1] J. F. Allard. *Propagation of Sound in Porous Media. Modelling Sound Absorbing Materials*. Elsevier, 1993.

[2] J. F. Allard and N. Atalla. *Propagation of Sound in Porous Media: Modelling Sound Absorbing Materials, Second Edition*. Wiley, 2009.

[3] N. Atalla, M. A. Hamdi, and R. Panneton. Enhanced weak integral formulation for the mixed (u,p) poroelastic equations. *J. Acoust. Soc. Am.*, 109(6):3065–3068, June 2001.

[4] N. Atalla, R. Panneton, and P. Debergue. A mixed displacement-pressure formulation for poroelastic materials. *J. Acoust. Soc. Am.*, 104(3):1444–1452, September 1998.

[5] C. Batifol, T. G. Zielinski, M. N. Ichchou, and M.-A. Galland. A finite-element study of a piezoelectric/poroelastic sound package concept. *Smart Mater. Struct.*, 16:168–177, 2007.

[6] A. Benjeddou. Advances in piezoelectric finite element modeling of adaptive structural elements: a survey. *Comput. Struct.*, 76:347–363, 2000.

[7] M. A. Biot. The theory of propagation of elastic waves in a fluid-saturated porous solid. *J. Acoust. Soc. Am.*, 28(2):168–191, 1956.

[8] N. Dauchez, S. Sahraoui, and N. Atalla. Convergence of poroelastic finite elements based on Biot displacement formulation. *J. Acoust. Soc. Am.*, 109(1):33–40, January 2001.

[9] P. Debergue, R. Panneton, and N. Atalla. Boundary conditions for the weak formulation of the mixed (u,p) poroelasticity problem. *J. Acoust. Soc. Am.*, 106(5):2383–2390, November 1999.

[10] C. R. Fuller, S. J. Elliott, and P. A. Nelson. *Active Control of Vibration*. Academic Press, 1996.

[11] D. Givoli. High-order local non-reflecting boundary conditions: a review. *Wave Motion*, 39:319–326, 2004.

[12] I. Harari. A survey of finite element methods for time-harmonic acoustics. *Comput. Methods Appl. Mech. Engrg.*, 195:1594–1607, 2006.

[13] T. Ikeda. *Fundamentals of Piezoelectricity*. Oxford University Press, 1990.

[14] P. Leroy, N. Atalla, A. Berry, and P. Herzog. Three dimensional finite element modeling of smart foam. *J. Acoust. Soc. Am.*, 126(6):2873–2885, 2009.

[15] G. A. Maugin. *Continuum Mechanics of Electromagnetic Solids*. Elsevier, 1988.

[16] A. Preumont. *Vibration Control of Active Structures*. Springer, 2002.

[17] J. N. Reddy. On laminated composite plates with integrated sensors and actuators. *Eng. Struct.*, 21:568–593, 1999.

[18] L. L. Thompson. A review of finite-element methods for time-harmonic acoustics. *J. Acoust. Soc. Am.*, 119(3):1315–1330, March 2006.

[19] T. G. Zielinski. Fundamentals of multiphysics modelling of piezo-poro-elastic structures. *Archives of Mechanics*, 62(5):343–378, 2010.

[20] T. G. Zielinski, M.-A. Galland, and M. N. Ichchou. Fully-coupled finite-element modelling of active sandwich panels with poroelastic core. *Journal of Vibration and Acoustics – Transactions of the ASME*, (submitted 2011).